Molecular Phylogenetics and Evolution 50 (2009) 31–43

Contents lists available at ScienceDirect

Molecular Phylogenetics and Evolution

journal homepage: www.elsevier.com/locate/ympev

Phylogeny of hoplocercine lizards (Squamata: Iguania) with estimates of relative divergence times

Omar Torres-Carvajal [a,b,*], Kevin de Queiroz [a]

[a] Department of Vertebrate Zoology, National Museum of Natural History, Smithsonian Institution, MRC 162, Washington, DC 20560, USA
[b] Escuela de Biología, Pontificia Universidad Católica del Ecuador, Avenida 12 de Octubre y Roca, Apartado 17-01-2184, Quito, Ecuador

ARTICLE INFO

Article history:
Received 25 April 2008
Revised 10 September 2008
Accepted 2 October 2008
Available online 11 October 2008

Keywords:
Andes
Chronophylogenetic
Hoplocercinae
Iguanidae
Neotropical
Phylogenetics
Relative divergence times

ABSTRACT

Hoplocercine lizards form a clade of 11 currently recognized species traditionally placed in three genera (*Enyalioides*, *Hoplocercus*, and *Morunasaurus*) that occur in the lowlands on both sides of the Andes between Panama and the Brazilian Cerrado. We analyze 11 mitochondrial and two nuclear loci using probabilistic methods and different partitioning strategies to (1) infer the phylogenetic relationships among species of Hoplocercinae, (2) examine amounts of inter- and intraspecific sequence divergence, (3) address monophyly of four species, (4) test previous phylogenetic hypotheses, and (5) estimate divergence times. Our preferred hypothesis places *H. spinosus* as the sister taxon to all other species of hoplocercines, with *M. annularis* nested within *Enyalioides*. Species with multiple samples are monophyletic except for *Enyalioides oshaughnessyi*, which is paraphyletic relative to an undescribed species of *Enyalioides*. All previously published phylogenetic hypotheses for hoplocercines are rejected. Monophyly of *Enyalioides* cannot be rejected and, consequently, the position of *Morunasaurus* remains unclear. The most recent common ancestor of Hoplocercinae probably occurred east of the Andes; western taxa included in our analyses originated from at least two separate colonizations whether pre- or post-dating vicariance resulting from uplift of the Andes.

1. Introduction

The neotropical lizard clade Hoplocercinae (sensu Schulte et al., 2003; =Hoplocercidae of Frost and Etheridge, 1989; =morunasaurs [informal] of Etheridge and de Queiroz, 1988) has been inferred as a basal clade within Iguanidae (Etheridge and de Queiroz, 1988; Schulte et al., 1998, 2003). Hoplocercinae includes 11 currently recognized species assigned to three taxa traditionally ranked as genera: *Enyalioides cofanorum*, *E. heterolepis*, *E. laticeps*, *E. microlepis*, *E. oshaughnessyi*, *E. palpebralis*, *E. praestabilis*, *Hoplocercus spinosus*, *Morunasaurus annularis*, *M. groi*, and *M. peruvianus*. These lizards inhabit lowlands between Panama and the Brazilian Cerrado on both sides of the Andes. In spite of the small size and potentially important basal phylogenetic position of this clade, the relationships among its species remain unclear. Moreover, natural history data for most species are scarce (e.g., Vitt and de la Torre, 1996) and major α-taxonomic work including the description of new species is needed (Wiens and Etheridge, 2003).

To date all attempts to infer the phylogeny of Hoplocercinae have been based on parsimony analyses of morphological characters. Etheridge and de Queiroz (1988) found that a greatly enlarged nasal scale (Etheridge, 1969) was a unique synapomorphy within Iguanidae supporting the monophyly of hoplocercines. Their analysis placed *E. laticeps* as the sister taxon to all other species in the group, with *Hoplocercus* nested within *Morunasaurus* and both nested within the spiny-tailed species of *Enyalioides*. More recently Wiens and Etheridge (2003) conducted analyses that yielded strikingly different topologies depending on how meristic characters were weighted. Their preferred weighting scheme had *Hoplocercus* and *Morunasaurus* forming the sister clade to *Enyalioides*.

In this paper, we infer phylogenetic relationships among species of Hoplocercinae based on multiple mitochondrial and nuclear loci, which are analyzed using probabilistic methods and different partitioning strategies. We then use our preferred phylogenetic tree to test statistically all previous hypotheses of relationships within Hoplocercinae. In addition, we use a recent Bayesian method that co-estimates phylogenies and divergence times (Drummond et al., 2006) to estimate divergence times for nodes within Hoplocercinae and use those estimates to address hypotheses concerning the biogeography of that clade.

2. Materials and methods

2.1. Character and taxon sampling

We obtained nucleotide (nt) sequences including both mitochondrial and nuclear DNA. Mitochondrial sequences extend from

* Corresponding author. Address: Escuela de Biología, Pontificia Universidad Católica del Ecuador, Avenida 12 de Octubre y Roca, Apartado 17-01-2184, Quito, Ecuador.
E-mail address: omartorcar@gmail.com (O. Torres-Carvajal).

1055-7903/$ - see front matter © 2008 Elsevier Inc. All rights reserved.
doi:10.1016/j.ympev.2008.10.002

the gene encoding subunit I of the protein NADH dehydrogenase (*ND1*) through the genes encoding $tRNA^{Ile}$, $tRNA^{Gln}$, $tRNA^{Met}$, subunit II of NADH dehydrogenase (*ND2*), $tRNA^{Trp}$, $tRNA^{Ala}$, $tRNA^{Asn}$, the origin of light-strand replication (O_L), $tRNA^{Cys}$, $tRNA^{Tyr}$, to the gene encoding subunit I of the protein cytochrome c oxidase (*COI*). Nuclear sequences include the recombination activating gene 1 (*RAG1*) and the brain-derived neurotrophic factor gene (*BDNF*).

We obtained new sequence data from 16 specimens representing nine species of Hoplocercinae including one specimen of a recently described species from southwestern Ecuador (*E. touzeti*), two specimens of *E. praestabilis*, and three specimens each of *E. heterolepis*, *E. oshaughnessyi*, and *E. laticeps*. We were unable to obtain sequence data from *Enyalioides cofanorum* and *Morunasaurus groi*. In addition, we used published sequences of *E. laticeps*, *Hoplocercus spinosus*, *Morunasaurus peruvianus*, and five outgroup taxa (Table 1). Complete mitochondrial and nuclear sequence data were obtained for 11 ingroup specimens (nine species) and all outgroups. Mitochondrial sequence data were obtained for additional ingroup taxa yielding an expanded mitochondrial dataset of 18 hoplocercine specimens (10 species) and all outgroups; this dataset was used to examine intra- and interspecific sequence divergence.

2.2. Laboratory protocols

Genomic DNA was extracted from liver or muscle using the DNeasy Tissue Kit® (Qiagen, Inc.). Amplification of DNA was conducted in a DNA Engine Dyad® Peltier Thermal Cycler (Bio-Rad) with a denaturation at 95 °C for 30 s, annealing at 50–57 °C for 30 s, and extension at 72 °C for 150 s for 35–40 cycles for mitochondrial genes. For amplification of *RAG1* annealing was at 55–60 °C, whereas for *BDNF* it was 50 °C and extension time was reduced to 50 s. Negative controls were run on all amplifications to check for contamination. Amplified products were purified with ExoSAP-IT (USB Corporation). Cycle-sequencing reactions were performed using ABI Prism Big Dye Terminator (Perkin-Elmer) chemistry with a denaturation at 96 °C for 10 s, annealing at 50 °C for 10 s, and extension at 60 °C for 4 min for 35 cycles. Sequencing reactions were run on a 3130xl Genetic Analyzer (Applied Biosystems). PCR and sequencing primers used in this study are listed in Table 2.

2.3. Alignment protocols

Editing and assembling of sequences were performed with Sequencher™ 4.2 (Gene Codes). DNA sequences were aligned in ClustalX 1.83 (Thompson et al., 1997) with default gap costs. Sequences encoding tRNAs were aligned by inferring secondary structures from primary structures of the corresponding tRNA genes based on standard tRNA models (Kumazawa and Nishida, 1993; Macey and Verma, 1997). Protein-coding sequences (i.e., *ND1*, *ND2*, *COI*, *BDNF*, *RAG1*) were translated into amino acids using MacClade 4.03 (Maddison and Maddison, 2001) for confirmation of alignment. A total of 123 mitochondrial sites corresponding to the 3′ ends of *ND1* and *ND2*, as well as some tRNA loops and the O_L loop included many gaps and could not be aligned unambiguously (e.g., several alignments were possible without changing the number of inferred sites) and were therefore excluded from the analyses. Aligned DNA sequences are available from the first author of this paper.

2.4. Model selection and phylogenetic analyses

We analyzed the data under maximum-likelihood (ML) and Bayesian approaches. After excluding those ingroup taxa for which nuclear sequence data were not obtained (Table 1), separate analyses were conducted for the following datasets: (1) mitochondrial data (mtDNA), (2) *BDNF*, (3) *RAG1*, (4) combined nuclear data (nDNA), and (5) combined mtDNA and nDNA (Table 3). Evolutionary models for each dataset and partition (combined datasets) were selected using Modeltest 3.7 (Posada and Crandall, 1998) under the Akaike information criterion (AIC), which avoids some limitations of the likelihood-ratio test (LRT), in particular the inability to compare non-nested models. Nonetheless, we also compared the AIC-selected models with the models selected by LRTs using Modeltest. If the models selected under both criteria for a particular dataset were different, we took additional steps not performed by Modeltest to evaluate whether the different selection criteria favored different models. These steps included conducting additional LRTs not computed automatically by Modeltest and adopting a standard significance level of $p = 0.05$ instead of $p = 0.01$ (Modeltest default). We also evaluated how well the AIC supported each LRT-selected model by comparing the difference in AIC values (Δ AIC) between the AIC- and LRT-selected models (when different) for each dataset, with Δ AIC < 2 being considered substantial support for both models (Burnham and Anderson, 2004).

For each dataset, a ML heuristic search was performed in PAUP*4.0b10 (Swofford, 2003) under a successive-approximations approach, in which parameter estimation and tree-searching are alternated until the same tree and model parameter estimates are found in successive iterations (Swofford et al., 1996; Sullivan et al., 2005). We first used the parameters estimated by Modeltest on a neighbor-joining tree to perform a heuristic search with 100 random addition-sequence replicates and tree bisection and reconnection (TBR) branch swapping. The resulting ML tree was then used to re-estimate the model and parameter values in Modeltest, which were used in a subsequent ML heuristic search in PAUP* with 100 random addition-sequence replicates. This process was repeated until the same model parameter estimates and tree were estimated successively. Support for individual nodes in the ML tree was assessed with non-parametric bootstrapping (BP) using GARLI 0.95 (Zwickl, 2006) with 100 pseudoreplicates, random starting trees, and parameters estimated from each resampled dataset under the model selected for the original dataset.

The five datasets mentioned above also were analyzed in MrBayes 3.1.2 (Huelsenbeck and Ronquist, 2001; Ronquist and Huelsenbeck, 2003) after partitioning the data as described in Table 4. Models for each partition were chosen in Modeltest as explained above (Table 3). In addition the combined (i.e., mtDNA + nDNA) dataset was analyzed both without partitioning and under two partition strategies (Table 4). These three strategies—a single model for all the data versus different models for each of four or seven partitions (Table 4)—were compared using Bayes factors. For a comparison involving models *a* and *b*, the Bayes factor (B_{ab}) is the ratio of the marginal likelihood (i.e., probability of the data given the model scaled by the model's prior probability and integrated over all parameter values) of model *a* to that of model *b* and represents a summary of the evidence provided by the data in favor of one model relative to the other (Kass and Raftery, 1995). Marginal likelihood values were estimated by computing the harmonic mean of the sampled likelihoods of each converged chain (Kass and Raftery, 1995; Raftery, 1996) in MrBayes. The harmonic mean estimators were interpreted on a logarithmic scale, with $2 \ln B_{ab}$ values > 5 considered as strong evidence favoring one model over the other (Kass and Raftery, 1995; Pagel and Meade, 2004; Raftery, 1996). For each dataset four independent analyses were performed, each consisting of 5×10^6 generations and five Markov chains with default heating values. Parameter values were estimated from the data and initiated with uniform priors except in the case of branch lengths, for which exponential priors were used. Trees were sampled every 1000 generations yielding 5000 trees saved per run. Convergence was assessed by plotting the log-likelihood scores per generation in

Table 1
Taxa included in this study, voucher specimen numbers, collecting localities, and GenBank accession numbers. Museum codes follow Leviton et al. (1985) except for Círculo Herpetológico de Panamá (CH), Museo de Zoología, Pontificia Universidad Católica del Ecuador (QCAZ), and Museo de Historia Natural, Universidad Nacional Mayor de San Marcos, Peru (MHNSM).

Species	Voucher specimen number and collecting locality	GenBank No.
Outgroup taxa		
Basiliscus plumifrons	UTA 44862	*BDNF*: AY987969 (Noonan and Chippindale, 2006)
	MVZ 204068; Costa Rica: Cartago: 2.5 km S Tapanti Bridge over Rio Grande de Orosi on road through Refugio Nacional Tapanti (9°44′41.6″N, 83°48′13.2″W), 1265 m	mtDNA: U82680 (Macey et al., 1997a) *RAG1*: AY662599 (Townsend et al., 2004)
Leiocephalus carinatus	UTA number not reported	*BDNF*: AY987970 (Noonan and Chippindale, 2006)
	No voucher; Bahamas: Marsh Harbour: Abaco (26°32′24″N, 77°8′60″W)	mtDNA: AF049864 (Schulte et al., 1998) *RAG1*: AY662598 (Townsend et al. 2004)
Liolaemus pictus	**BYU 48406**; Chile: Los Lagos: Estaquitas (41°26′54″S, 73°43′37″W)	*BDNF*: AY987974 (Noonan and Chippindale, 2006)
	MIC 1108 (field number); Argentina: Neuquén: 3 km W Ardillas 1475 m	mtDNA: AF099226 (Schulte et al., 2000)
	MVZ 162076; Argentina: Rio Negro: Bariloche, Rio Castano Overo, 44 km W Bariloche (41°38′60″S, 71°47′24″W)	*RAG1*: AY662595 (Townsend et al., 2004)
Oplurus cuvieri	**MVZ 238791**; Comoros: Grand Comore: coastal cliffs 1.0 km NE (by air) Mtsamdou (11°35.9′S, 43°22.4′E), 20 m	*BDNF*: AY987971 (Noonan and Chippindale, 2006)
	MVZ-RM10468B; Madagascar	mtDNA: U82685 (Macey et al., 1997a) *RAG1*: AY662601 (Townsend et al., 2004))
Phrynosoma mccalli	**CAS 229923**; USA: Arizona: Yuma Co.: Barry M. Goldwater Air Force Base (32°29′20″N, 114°27′13″W)	*BDNF*: DQ385328 (Leaché and McGuire., 2006)
	MVZ 230681; USA: California: San Diego Co.: 0.3 mi. N Old Springs Road on Hwy S 22 (33°15′42″N, 116°17′53″W), 180 m	mtDNA: AY662534 (Townsend et al., 2004) *RAG1*: AY662590 (Townsend et al., 2004)
Ingroup taxa		
Enyalioides heterolepis	**CH 5328**; Panama: Coclé: El Santísimo (08°41′60″N, 80°28′00 ″W), 427 m	mtDNA: EU586745 (this study)
	CH 5629; Panama: Darién: trail to Serranía del Pirre, between Cana and camp at Serranía, 900 m	mtDNA: EU586746 (this study)*BDNF*: EU586760 (this study)*RAG1*: EU586771 (this study)
	QCAZ 6192; Ecuador: Esmeraldas: Durango (00°53′00″N, 78°48′00″ W), <300 m	mtDNA: EU586744 (this study) *BDNF*: EU586759 (this study) *RAG1*: EU586770 (this study)
Enyalioides laticeps	**LSUMZ 13573**; Brazil: Acre: ~5 km N Porto Walker (08°15′31″S, 72°46′37″W)	mtDNA: AF528719 (Schulte et al., 2003)
	KU 222164; Peru: Loreto: San Jacinto (02°18′44.8″S, 75°51′46″W), 180 m	mtDNA: EU586747 (this study) *BDNF*: EU586761 (this study) *RAG1*: EU586772 (this study)
	QCAZ 6035; Ecuador: Orellana: Pontificia Universidad Católica del Ecuador research station at Yasuni National Park (00°40′32″S, 76°24′19″W)	mtDNA: EU586748 (this study) *BDNF*: EU586762 (this study) *RAG1*: EU586773 (this study)
	QCAZ 6588; Ecuador: Sucumbíos: Tarapoa (00°7′60″S, 76°25′00″W), 280 m	**mtDNA: EU586749** (this study)
Enyalioides microlepis	**KU 222163**; Peru: Loreto: San Jacinto (02°18′44.8″S, 75°51′46″W), 180 m	mtDNA: EU586750 (this study) *BDNF*: EU586763 (this study) *RAG1*: EU586774 (this study)
Enyalioides oshaughnessyi	**QCAZ 6866**; Ecuador: Esmeraldas: Bilsa Ecological Reserve (00°37′N, 79°51′W), 225 m	mtDNA: EU586751 (this study) *BDNF*: EU586764 (this study) *RAG1*: EU586775 (this study)
	QCAZ 6899; Ecuador: Los Ríos: Jauneche Scientific Station (1°10′0″S, 79°40′0″W), 50 m	mtDNA: EU586752 (this study)
	QCAZ 6671; Ecuador: Esmeraldas: Alto Tambo, Río Balthazar (0°52′0N, 78°31′60W), 556 m	mtDNA: EU586753 (this study)
Enyalioides palpebralis	**MHNSM 24663**; Peru: Cuzco: Provincia La Convención: Distrito Echarate, 399 m	mtDNA: EU586754 (this study) *BDNF*: EU586765 (this study) *RAG1*: EU586776 (this study)
Enyalioides praestabilis	**QCAZ 4113**; Ecuador: Pastaza: Shell Mera (1°30′S, 78°2′60″W), 1123 m	mtDNA: EU586756 (this study) *BDNF*: EU586766 (this study) *RAG1*: EU586777 (this study)
	QCAZ 5580; Ecuador: Napo: Río Hollín (0°42′12″S, 77°43′4.7″W)	**mtDNA: EU586755** (this study)
Enyalioides touzeti	**EPN 10306**; Ecuador: Azuay: Finca La Envidia, Santa Marta hill (3°3′0′S, 79°41′25″W), 433 m	mtDNA: EU586757 (this study) *BDNF*: EU586767 (this study) *RAG1*: EU586778 (this study)
Hoplocercus spinosus	**MZUSP 907931**; Brazil: Mato Grosso: General Carneiro (15°41′60″S, 52°45′00″W) 347 m	mtDNA: U82683 (Macey et al., 1997a) *RAG1*: AY662592 (Townsend et al., 2004)
	MZUSP 95990; Brazil: Mato Grosso: Sapezal (13°23′54″S, 59°00′21″W)	*BDNF*: EU586769 (this study)

(*continued on next page*)

Table 1 (*continued*)

Species	Voucher specimen number and collecting locality	GenBank No.
Morunasaurus annularis	**QCAZ 7820**; Ecuador: Pastaza: Upper Bobonaza river (1°30′10.6″S, 77°52′44″W), 676 m	mtDNA: EU586758 (this study) *BDNF*: EU586768 (this study) *RAG1*: EU586779 (this study)
Morunasaurus peruvianus	**MVZ 163062**; Peru: Amazonas: Rio Cenepa, ridge on N side at headwaters of Rio Kagka (4°22′59.9″S, 78°11′48″W)	mtDNA: AF528720 (Schulte et al., 2003)

Table 2
Primers used for amplification and sequencing reactions.

Primer 5′–3′ sequence	Gene	Source
Forward		
CGATTCCGATATGACCARCT	ND1	Kumazawa and Nishida (1993)
GCCCCATTTGACCTCACAGAAGG	ND1	Macey et al. (1998)
ACAGAAGCCGCAACAAAATA	ND2	Macey et al. (1997b)
TGACAAAAACTAGCCCC	ND2	Macey et al. (1999)
CACAYTTTTGACTNCCAGAAGT	ND2	Torres-Carvajal et al. (2006)
AAGGATTACTTTGATAGAGT	$tRNA^{Ile}$	Macey et al. (1997b)
AAGGGNTACTTTGATAGAGT	$tRNA^{Ile}$	Schulte et al. (2003)
AAGCTTTCGGGCCCATACC	$tRNA^{Met}$	Macey et al. (1997b)
GGGCCCATACCCCNAANATG	$tRNA^{Met}$	This study
AACCAAGRGCCTTCAAAG	$tRNA^{Trp}$	Schulte et al. (2003)
GACCATCCTTTTCCTKACTATGGTTATTTCATACTT	BDNF	Leaché and McGuire (2006)
ATGTCCATGAGGGTCCGGCGCC	BDNF	J. Schulte (personal communication)
TCTGAATGGAAATTCAAGCTGTT	RAG 1	Townsend et al. (2004)
CAAAGTRAGATCACTTGAGAAGC	RAG 1	J. Schulte (personal communication)
AAGCAATTCCCCATGTGA	RAG 1	This study
Reverse		
AGRGTGCCAATGTCTTTGTGRTT	COI	Macey et al. (1997b)
GCTATGTCTGGGGCTCCAATTAT	COI	Weisrock et al. (2001)
ACTATTCCRGCYCAGGCACCRAAGA	COI	J. Schulte (personal communication)
ATTTTTCGTAGTTGGGTTTGRTT	ND2	Macey et al. (1997b)
ATGGCTAGTGTGTTTATTTCTA	ND2	Schulte and de Queiroz (2008)
AAAYTRTCTGRGTTGCAWTCAG	$tRNA^{Ala}$	This study
TTGGGTGTTTAGCTGTTAA	$tRNA^{Asn}$	Macey et al. (1997b)
CTGGTTTGGGTAGTTAGCTGTTAA	$tRNA^{Asn}$	Torres-Carvajal et al. (2006)
GGTATGAGCCCGATAGCTT	$tRNA^{Met}$	Macey et al. (1997b)
CTATCTTCCCCTTTTAATGGTCAGTGTACAAAC	BDNF	Leaché and McGuire (2006)
GCTTCAGTTGGCCTTTNGG	BDNF	J. Schulte (personal communication)
TGGTCCATGNACTGGGT	RAG 1	This study
GTGTTGACTCTGATT	RAG 1	This study
ACTTGYAGCTTGAGTTCTCTTAGRCG	RAG 1	J. Schulte (personal communication)
GGCCTGANCCCTTWCCTTGCAT	RAG 1	J. Schulte (personal communication)
CATTTTTCAAGGGTGGTTTCCACTC	RAG 1	J. Schulte (personal communication)

Table 3
Datasets and data partitions used in this study. Number of nucleotides (nt), selected model under the Akaike information criterion (AIC) and likelihood-ratio tests (LRTs), AIC difference between AIC- and LRT-selected models (Δ AIC), as well as number of unique site patterns (USP), variable sites (VS) and parsimony-informative sites (PIS) are indicated for each dataset and partition.

Dataset/partition	nt	Selected model		Δ AIC	USP	VS	PIS
		AIC	LRTs				
Datasets							
mtDNA	1650	GTR + I + G	TVM + I + G	5.87	750	911	667
BDNF	610	TIM + I + G	K80 + G	4.76	52	63	19
RAG 1	1074	HKY + G	HKY + G	—	200	302	105
nDNA[a]	1684	HKY + G	HKY + G	—	220	365	124
mtDNA + nDNA	3457	GTR + I + G	GTR + I + G	—	894	1276	791
Partitions for mtDNA and nDNA datasets							
tRNAs	506	TVM + I + G	TVM + G	0.50	186	215	137
Protein-coding mtDNA							
1st codon	382	TVM + I + G	TVM + G	0.16	200	216	152
2nd codon	381	TVM + G	HKY + G	18.07	114	125	87
3rd codon	381	TrN + I + G	HKY + I + G	1.43	338	355	291
Protein-coding nDNA							
1st codon	561	K81uf + G	HKY + G	1.39	79	92	27
2nd codon	561	HKY + I	HKY + G	0.14	71	73	26
3rd codon	562	HKY + G	K80 + G	1.19	139	200	71

[a] *BDNF* + *RAG1*.

Table 4
Partition strategies for five datasets analyzed under Bayesian inference (nDNA = *BDNF* + *RAG 1*).

Dataset	Number of partitions	Partitions
mtDNA	4	tRNAs, 1st, 2nd and 3rd codon positions of protein-coding genes
BDNF	3	1st, 2nd, and 3rd codon positions
RAG1	3	1st, 2nd, and 3rd, codon positions
nDNA	3	1st, 2nd, and 3rd codon positions
mtDNA + nDNA	4	tRNAs; 1st, 2nd, and 3rd codon positions of mitochondrial and nuclear protein-coding genes combined
mtDNA + nDNA	7	tRNAs; 1st, 2nd, and 3rd codon positions of mitochondrial protein-coding genes; 1st, 2nd, and 3rd codon positions of nuclear genes

TRACER 1.4 (Rambaut and Drummond, 2007). Additionally, the standard deviation of the partition frequencies and the potential scale reduction factor (Gelman and Rubin, 1992) were used as convergence diagnostics for the posterior probabilities of bipartitions and branch lengths, respectively; these diagnostics were obtained by summarizing all four runs for each dataset. Adequacy of mixing was assessed by examining the acceptance rates for the parameters in MrBayes and the effective sample sizes (ESS) in TRACER. After discarding those generations prior to convergence (i.e., burn-in), trees of the remaining generations were used to estimate posterior probabilities (PP) of bipartitions by constructing a 50% majority-rule consensus tree.

Bayesian inference also was conducted in the program BayesPhylogenies (Pagel and Meade, 2004) under the mixture-models approach using the combined mitochondrial and nuclear dataset. This approach accommodates heterogeneity across sites in the patterns of gene-sequence evolution without a priori partitioning by allowing more than one model (i.e., rate [Q] matrix) to be applied to each site in the alignment. The individual likelihoods of the various models at each site are then summed, after weighting the models by the probability that they apply to that site, which can be estimated from the data (Pagel and Meade, 2004, 2005). The model of evolution (i.e., number of Q matrices, each conforming to the GTR + Γ model) was selected using reversible jump Markov Chain Monte Carlo (Huelsenbeck et al., 2004) as implemented in a test version of BayesPhylogenies provided by its authors. One run consisting of 10^7 generations and four Markov chains was conducted in BayesPhylogenies. Trees were sampled every 1000 generations resulting in 10,000 saved trees; convergence and ESSs were assessed in TRACER. The trees remaining after "burn-in" were used to estimate posterior probabilities of bipartitions by constructing a 50% majority-rule consensus tree.

2.5. Hypothesis tests

Monophyly of *Enyalioides* and alternative phylogenetic hypotheses presented by previous authors (Fig. 1) were tested against the ML tree obtained from the analysis of a combined mtDNA and nDNA dataset. This dataset, which we call the pruned combined dataset, included only one sample per species, excluded the new *Enyalioides* species, and was analyzed following the same protocols described above. The alternative topologies (i.e., monophyly of *Enyalioides* and hypotheses from the literature) were constructed

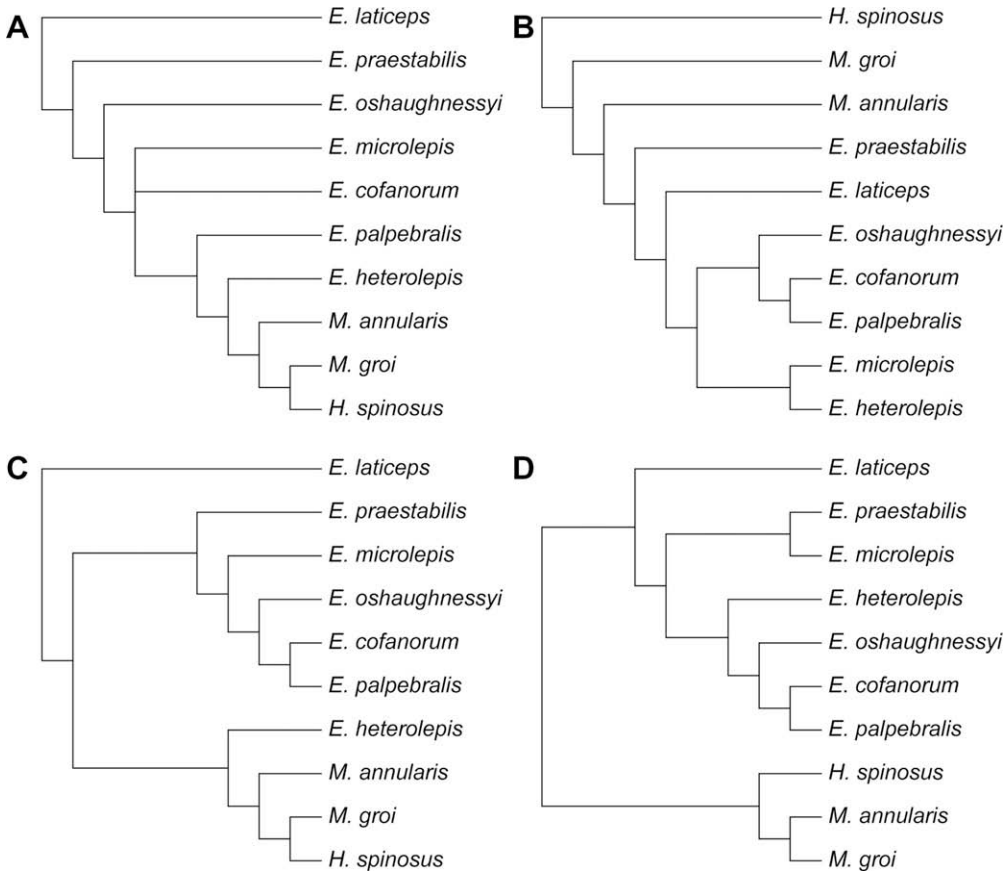

Fig. 1. Four hypotheses of phylogenetic relationships among hoplocercine lizards. (A) Etheridge and de Queiroz (1988); (B–D) Between-state, between-character, and mixed scaling, respectively (Wiens and Etheridge, 2003). *H.*, *Hoplocercus*; *M.*, *Morunasaurus*; *E.*, *Enyalioides*.

in MacClade 4.03 after excluding taxa for which we lacked either mtDNA or nDNA data (i.e., *Enyalioides cofanorum*, *Morunasaurus groi*, and *M. peruvianus*). To test the monophyly of *Enyalioides* we obtained the maximum-likelihood tree under that constraint following the successive-approximations approach described above. We conducted Shimodaira–Hasewaga (SH) and approximately unbiased (AU) tests (Shimodaira and Hasegawa, 1999; Shimodaira, 2002, respectively) using CONSEL 0.1i (Shimodaira and Hasegawa, 2001). The likelihood scores used in both tests were obtained in PAUP* by re-estimating parameter values for each alternative topology.

In addition, we used a Bayesian approach to tree topology tests by determining the posterior probability of each alternative topology. For these tests we conducted a Bayesian analysis of the pruned combined dataset using the same models and protocols (see above) applied to the full (i.e., without pruning any taxa) partitioned combined dataset (Tables 3 and 4). The resulting post-burn-in trees were loaded into PAUP* and then filtered using each alternative topology to determine the frequency (i.e., posterior probability) of that topology within the sample. If the alternative topology was not within the 95% credible set of trees, we considered it rejected by the observed data.

2.6. Sequence divergence and species monophyly

To address intra- and interspecific sequence divergence, as well as species monophyly in some hoplocercine species, we used an expanded mitochondrial dataset of 18 hoplocercine specimens representing 10 species (Table 1). Sequence variation was assessed with maximum-likelihood corrected distances, which were obtained in PAUP* under the same model selection strategy used in the phylogenetic analyses. Species monophyly was addressed by performing a maximum-likelihood phylogenetic analysis following the protocols described above.

2.7. Chronophylogenetic analyses

Chronophylogenetic analyses (i.e., co-estimation of rates, divergence times, and phylogeny) were conducted under the Bayesian framework implemented in BEAST 1.4.5 (Drummond and Rambaut, 2007) using the unpartitioned and seven-partition (Table 4) combined datasets (see Supplementary material for XML files). The analyses were conducted under a model with uncorrelated substitution rates among branches and the rate for each branch independently drawn from an underlying lognormal distribution (Drummond et al., 2006). Default parameter priors were used except for the *mean of branch rates* parameter (ucld.mean), which was fixed to 1.0 reflecting the absence of calibration dates and resulting in time being measured in units that have been arbitrarily chosen so that 1 time unit corresponds to the mean time required for the accumulation of 1 substitution per site (Drummond et al., 2006; Drummond and Rambaut, 2007). For each dataset we performed three independent 10^7 generation runs with random starting trees, sampling every 1000 generations. Results were analyzed in TRACER to assess convergence and ESSs for all parameters. Remaining parameters were summarized onto the maximum-credibility tree (i.e., the tree with the maximum product of the posterior clade probabilities) resulting from the analysis of each of the unpartitioned and the partitioned combined datasets. The effects of data partitioning on this Bayesian method for co-estimating phylogeny and divergence times were assessed with Bayes factors and by comparing the estimated rates and relative times between the unpartitioned and the partitioned datasets. In addition, a chronophylogenetic analysis was conducted without the outgroups to estimate the position of the root for Hoplocercinae independently.

Although internal and nearby external calibrations were not available, the rate of evolution for the same mitochondrial region used in this study has been estimated to be 0.65% change per lineage per million years (my) for iguanian lizards in the distantly related *Laudakia caucasia* species group (Macey et al., 1998). Treating this value as a rough estimate of an average rate for hoplocercines, we used the expanded, unpartitioned mitochondrial dataset (18 hoplocercine taxa) and the same protocols described in the previous paragraph to perform a chronophylogenetic analysis in which the prior value for the *mean of branch rates* parameter was set to 0.0065, with lower and upper boundaries of 0.006 and 0.007, respectively. Default priors were used for the remaining parameters.

3. Results

We obtained a total of 3457 (aligned) sites of mitochondrial and nuclear DNA. Mitochondrial sequences ranged between 1730 and 1748 nt, whereas nuclear sequences included 1041–1074 nt For *RAG1* and 610 nt for *BDNF*. Numbers of unique site patterns, variable characters, and parsimony-informative characters are given in Table 3.

3.1. Model selection

Models selected by the AIC and LRTs for the various genes (or contiguous fragments of DNA) and partitions thereof are given in Table 3. The same model was selected under both selection criteria for datasets *RAG1*, nDNA, and mtDNA + nDNA. For the remaining datasets, the AIC generally selected a more complex model than did the LRTs as commonly observed in other datasets (Ripplinger and Sullivan, 2008).

For the nDNA/2nd codon position partition, LRTs selected the HKY + G model, whereas AIC favored HKY + I; however, when we tested for invariant sites (I) before testing for rate heterogeneity (G), the reverse of Modeltest's order, HKY + I was selected. Moreover, the likelihood-ratio was slightly greater for the latter test indicating slightly better support for HKY + I. For the mtDNA/2nd codon position partition, LRTs selected the HKY + G model, whereas AIC selected the TVM + G model; however, these models were not compared by Modeltest. We conducted a LRT comparing these models and TVM + G was strongly favored over HKY + G ($p < 0.0001$). For the mtDNA dataset, LRTs selected the TVM + I + G model, whereas AIC favored the GTR + I + G; however, if we adopt the standard 0.05 significance level (Modeltest's default is 0.01), equal transition rates are rejected ($p = 0.046$) and the resulting model is GTR + I + G. Similarly, for the nDNA/3rd codon position partition, LRTs adopting the 0.05 significance level would select the same model as AIC (HKY + G) by rejecting equal base frequencies ($p = 0.041$). For the *BDNF* dataset the LRTs favored K80 + G and AIC selected K81uf + I + G; however, if we adopt a 0.05 level of significance, LRTs select HKY + I + G. In this case and all remaining cases (tRNAs, mtDNA/1st codon position, mtDNA/3rd codon position, nDNA/1st codon position) the models selected by AIC versus LRTs are nested, differ by a single parameter, and are both well supported (i.e., Δ AIC < 2).

3.2. Hoplocercine phylogeny

For each of the five datasets analyzed in this study, ML ingroup topologies were identical to those obtained under Bayesian analyses (Figs. 2 and 3), in which convergence was reached prior to 500,000 generations, and the first 500 sampled generations were discarded as "burn-in." The *BDNF* dataset contained the smallest numbers of variable characters and unique site patterns (Table 3) and not surprisingly it yielded the least resolved phylogenetic tree,

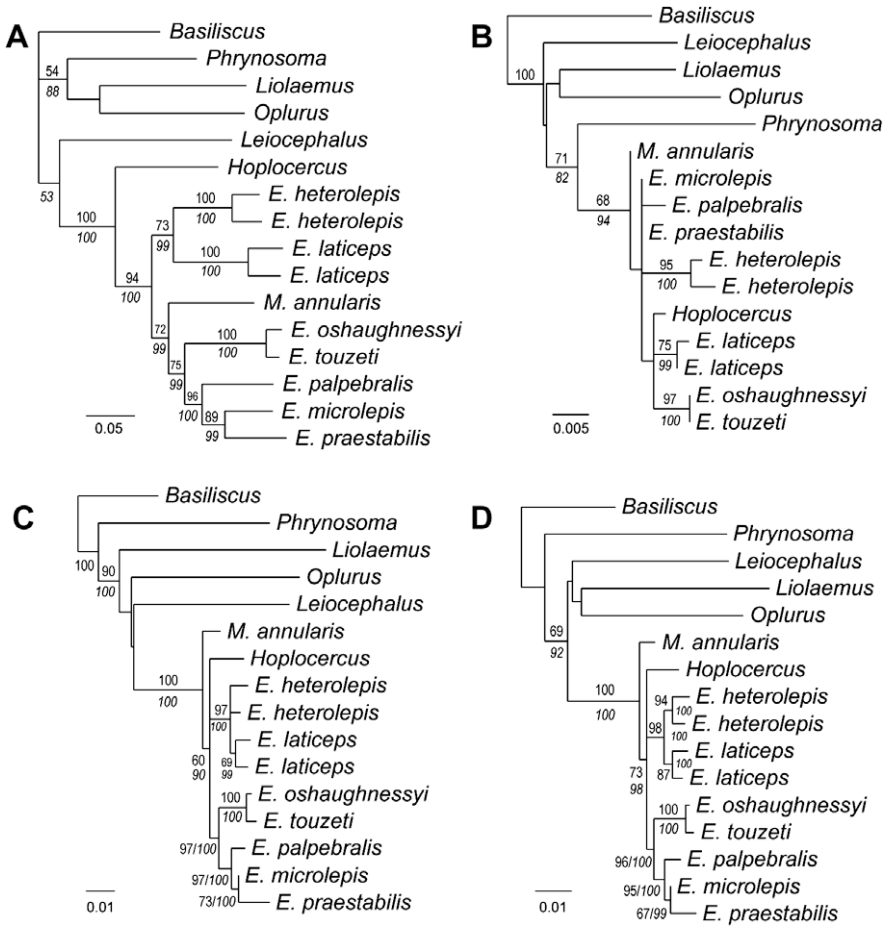

Fig. 2. ML trees of four datasets. (A) mtDNA; (B) BDNF; (C) *RAG1*; (D) BDNF + *RAG1*. Bootstrap support and Bayesian posterior probability values (italicized) > 50 are indicated.

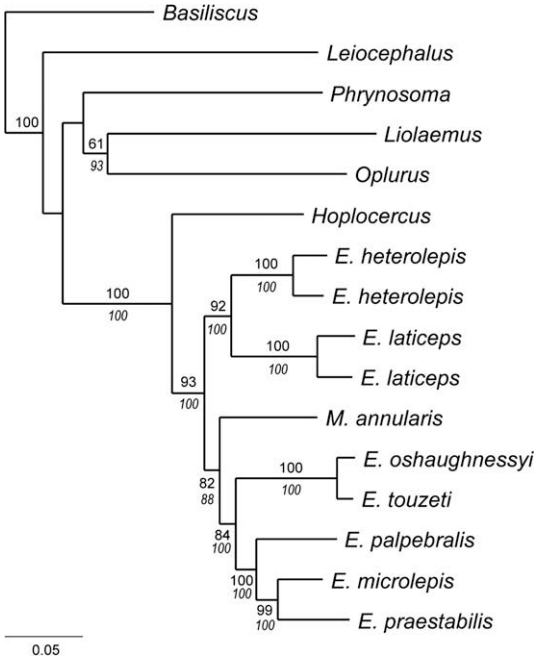

Fig. 3. ML tree of the combined mitochondrial and nuclear dataset. Maximum-likelihood bootstrap support and Bayesian posterior probability (italics) values > 50 are indicated. The ingroup posterior probability values were obtained under two partition strategies applied to the combined dataset (Table 4) and were identical for the two strategies. The single outgroup posterior probability value > 50 supporting *Liolaemus* and *Oplurus* as sister taxa was obtained under the seven-partition strategy.

with strong support only for the monophyly of conspecific samples, as well as the relationship between *E. oshaughnessyi* and the undescribed *Enyalioides* species (Fig. 2b). The remaining datasets were largely congruent with regard to the ingroup topology, except for the placement of *Hoplocercus spinosus* and *Morunasaurus annularis*. The mitochondrial and combined (i.e., mtDNA and nDNA) datasets placed *H. spinosus* as the sister taxon to all other species of hoplocercines, with *M. annularis* being the sister taxon to a clade composed of *E. palpebralis*, *E. microlepis*, *E. praestabilis*, *E. oshaughnessyi*, and *E. touzeti*. (Figs. 2a and 3). In contrast, the nuclear datasets placed *M. annularis* as the sister taxon to all other hoplocercines, with *H. spinosus* either as part of a clade also containing *E. laticeps*, *E. oshaughnessyi*, *and E.* sp (Fig. 2b) or in a more basal position within a clade containing all of the *Enyalioides* species (Fig. 2c and d).

Bayes factors strongly favored partitioning the combined dataset; moreover, the seven-partition strategy was favored over the four-partition one (Table 5). Nonetheless, both partition strategies yielded identical ingroup tree topologies and posterior probability

Table 5
Bayes factor comparisons (above diagonal) between the unpartitioned combined dataset and two-partition strategies along with numbers of free parameters (diagonal) and differences in numbers of free parameters (below diagonal). Details of both partition strategies are given in Table 4.

	Unpartitioned	Four-partitions	Seven-partitions
Unpartitioned	6	769	2363
Four-partitions	13	19	1594
Seven-partitions	20	7	26

values. The clade Hoplocercinae and all of its subclades were strongly supported (PP = 100), except for the least inclusive clade (LIC) containing *M. annularis* and *E. praestabilis* (PP = 88) (Fig. 3). Similarly, using the unpartitioned combined dataset, ML bootstrap values of 92 or higher supported all ingroup clades except for the LIC containing *M. annularis* and *E. praestabilis* (BP = 82) and the LIC containing *E. oshaughnessyi* and *E. praestabilis* (BP = 84).

Convergence in the mixture-models analysis was reached prior to 100,000 generations; accordingly, the first 1000 sampled generations were discarded as "burn-in." A single model, three *Q* matrices (3*Q*), was visited by the reversible jump Markov chain in all sampled post-burn-in generations. Resulting posterior probabilities of ingroup bipartitions were very similar to those obtained in the *a priori* partitioned Bayesian analysis of the same (mtDNA + nDNA) dataset (Fig. 3 and Table 4); the only difference was that the support for the LIC containing *M. annularis* and *E. praestabilis* was slightly lower in the mixture-models analysis (PP = 86).

3.3. Tests of alternative hypotheses

When trees corresponding to previously proposed morphology-based hypotheses of hoplocercine relationships (Fig. 1) were tested against the ML tree using the unpartitioned, combined mtDNA + nDNA dataset presented in this paper, all were decisively rejected with SH and AU tests ($p < 0.001$; Table 6). Because paraphyly of *Enyalioides* relative to *Hoplocercus* or *Morunasaurus* is suggested by some of our analyses (Figs. 2 and 3), we also compared the ML tree for our combined dataset with a tree constrained to have *Enyalioides* as a monophyletic group. This alternative tree topology could not be rejected by SH or AU tests ($p = 0.649$ and 0.116, respectively; Table 6).

The post-burn-in sample of 18,000 trees from the Bayesian analysis of the pruned combined dataset contained six tree topologies, which had posterior probability estimates ranging from <0.001 to 0.877. None of the previously proposed hypotheses (Fig. 1) were present in the sample of post-burn-in tree topologies. In contrast, monophyly of *Enyalioides* was supported by two sampled tree topologies ranked as 2nd (PP = 0.090) and 4th (PP < 0.001). Because the topology ranked as 2nd was within the 95% credible set of trees, monophyly of *Enyalioides* could not be rejected.

3.4. Sequence divergence and species monophyly

Sequence divergence between hoplocercines and the outgroups ranged (ML-corrected/uncorrected distance values) from 0.465/0.213 (*Enyalioides microlepis* and *Basiliscus plumifrons*) to 0.766/0.263 (*E. oshaughnessyi* and *Liolaemus pictus*). Interspecific sequence divergence within Hoplocercinae ranged from 0.03/0.03 (*E. oshaughnessyi* and *E. touzeti*) to 0.395/0.196 (*E. laticeps* and *Hoplocercus spinosus*); however, most ML-corrected distance values were above 0.15 (Fig. 4; mean = 0.277 ± 0.063 SD). For species represented by multiple samples (localities) intraspecific sequence divergences were 0.025–0.068/0.025–0.062 for *E. heterolepis* ($N = 3$), 0.017–0.081/0.017–0.071 for *E. laticeps* ($N = 4$), 0.003–0.052/0.003–0.048 for *E. oshaughnessyi* ($N = 3$), and 0.035/0.034 for *E. praestabilis* ($N = 2$). All species with multiple samples, except *E. oshaughnessyi*, were strongly supported as monophyletic groups by a maximum-likelihood analysis (Fig. 5).

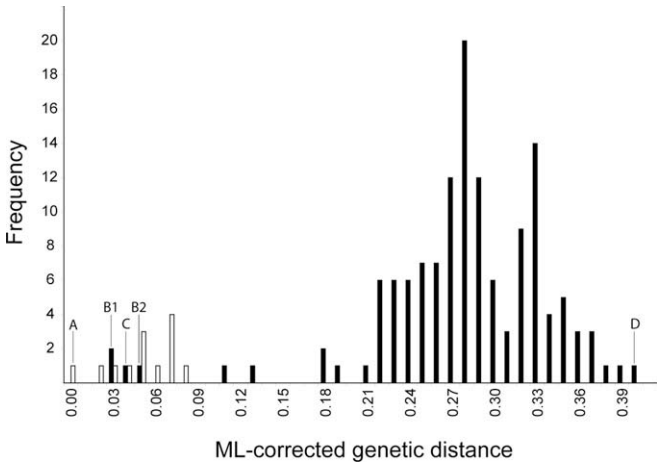

Fig. 4. Histogram illustrating the distribution of ML-corrected distances among 18 hoplocercine individuals representing 10 species based on the mitochondrial DNA sequence data. White bars indicate intraspecific comparisions; black bars correspond to interspecific comparisons. (A) distance between two specimens of *E. oshaughnessyi* (15 and 16 in Fig. 5); (B1) distance between *E. touzeti* and each of the two former specimens; (B2) distance between *E. touzeti* and a third specimen of *E. oshaughnessyi* (13 in Fig. 5); (C) distance between *Morunasaurus annularis* and *M. peruvianus*; (D) distance between *E. laticeps* and *Hoplocercus spinosus*.

3.5. Rate and divergence time estimates

Convergence in all chronophylogenetic analyses was reached prior to 10^6 generations; therefore, the first 1000 of the 10,000 sampled generations in each run were discarded as "burn-in". Ingroup topologies obtained from analyses of the unpartitioned and partitioned combined datasets under the uncorrelated lognormal model were identical to the topology obtained under time-reversible ML and Bayesian approaches (Figs. 3 and 6). All clades within Hoplocercinae had the maximum posterior probability (1.00) except for the least inclusive clade containing *Morunasaurus* and *E. oshaughnessyi* (0.98 in both cases). Values of relative divergence time estimates (node heights) were markedly different between the two combined datasets, with 95% highest posterior density (HPD) intervals overlapping only for the most recent nodes (Fig. 6). In general, divergence time estimates were larger for the partitioned dataset than they were for the unpartitioned dataset, with greater differences for older nodes. Both the unpartitioned and partitioned combined datasets yielded *ucld.stdev* estimated values close to 0 (95% HPD intervals = 0.048–0.243 and 0.059–0.273, respectively), indicating that the data are close to being clocklike. The root position for the ingroup inferred by the chronophylogenetic analysis without outgroups was identical to that inferred using time-reversible methods with outgroup rooting.

Based on the rate of 0.65% change per lineage per million years proposed by Macey et al. (1998), treated here as a rough estimate of the average rate for our distantly related taxon, the rough estimated age of Pan-Hoplocercinae was 56.35 my (95% HPD interval = 45.37–68.03 my). Rough estimated ages for Hoplocercinae

Table 6
Results of hypothesis tests. For the Shimodaira–Hasegawa (SH) and approximately unbiased (AU) tests, the observed difference in likelihood score (δ −lnL) between each alternative hypothesis and the ML tree resulting from analysis of the combined dataset (mtDNA + nDNA) along with the *p*-values for each test are presented. For the Bayesian approach, presence (+) or absence (−) of each alternative topology within the 95% credible set of trees (CS) is indicated.

Alternative hypothesis	δ −lnL	*p*-Value		CS
		SH	AU	
Etheridge and de Queiroz (1998) (Fig. 1d)	100.5	0	3e-04	−
Wiens and Etheridge (2003)				
Between-state scaling tree (Fig. 1a)	108.9	3e-01	8e-05	−
Between-character scaling tree (Fig. 1b)	64.6	0	7e-01	−
Mixed scaling tree (Fig. 1c)	59.5	1e-01	3e-01	−
Monophyly of *Enyalioides* (Fig. 1e)	4.7	0.649	0.116	+

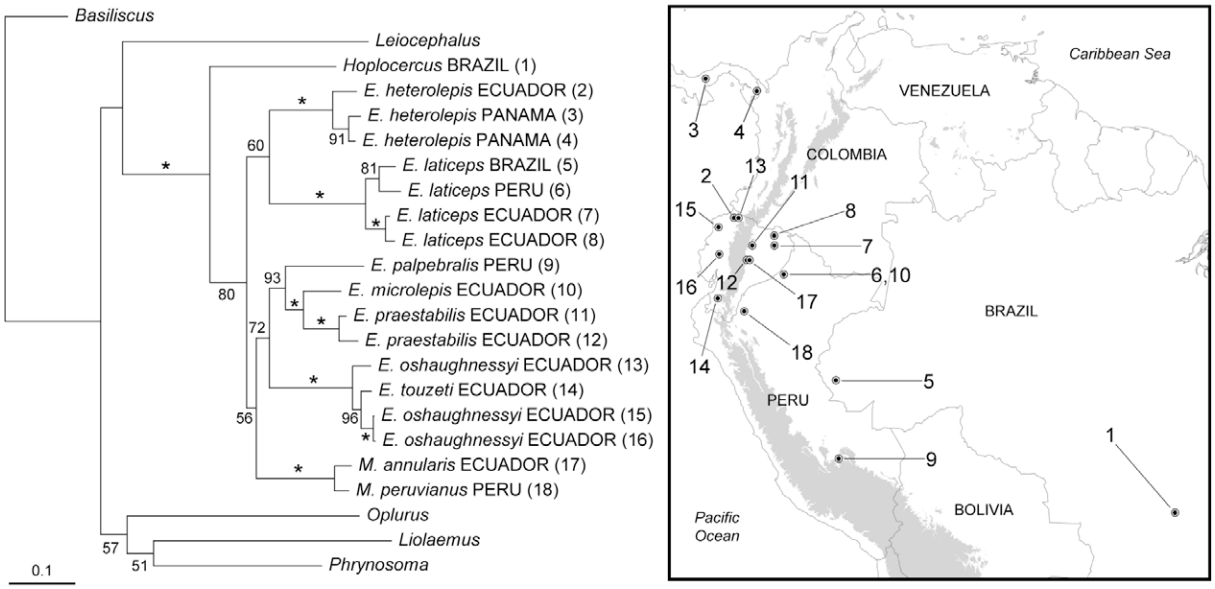

Fig. 5. ML tree (left) for a mitochondrial dataset including 18 hoplocercine samples from different localities indicated in the map (right). The name of the country where each sample was collected is indicated after each taxon name followed by a number in parentheses that corresponds to the locality number in the map. Bootstrap support values > 50 are indicated in the tree; asterisks correspond to values of 100.

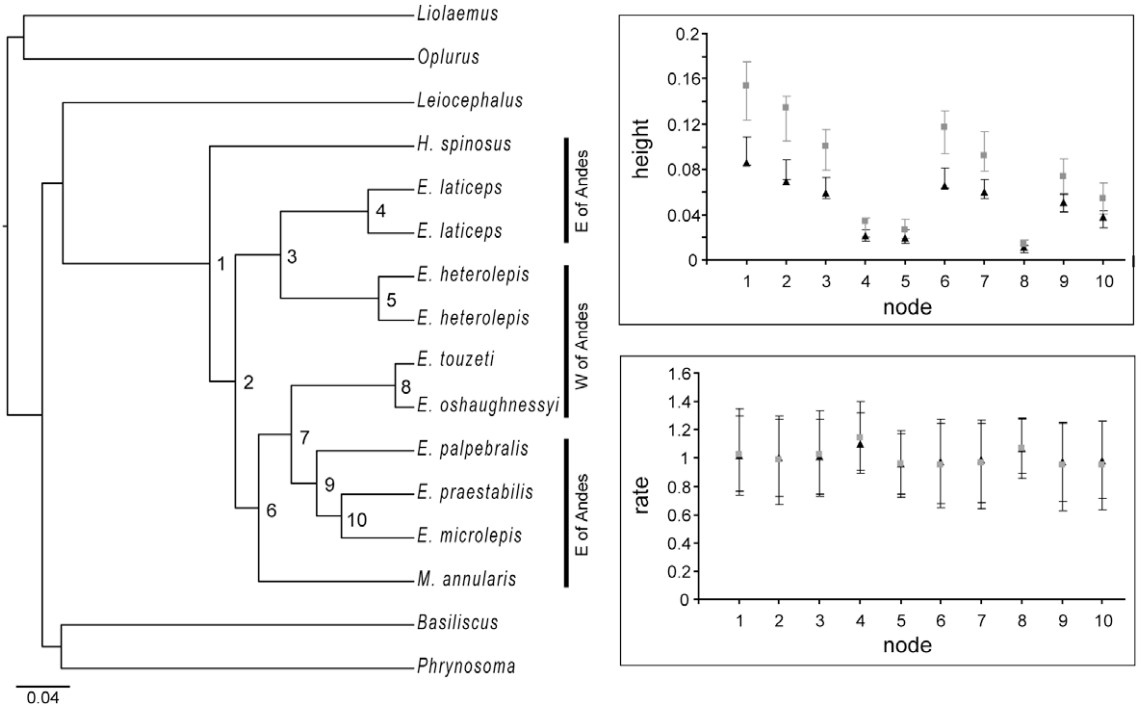

Fig. 6. Maximum credibility tree (left) inferred from the analysis of the partitioned combined dataset under uncorrelated, log normally distributed rates; branch lengths are in expected substitutions per site. Black vertical bars indicate the general geographic distribution of each species relative to the Andes Mountains. Estimates of node heights (i.e., divergence times; above right) and rates (below right) are presented with their 95% HPD intervals; estimates based on both the partitioned (grey squares) and unpartitioned (black triangles) combined datasets are shown. Node numbers in the tree correspond to node numbers in both the plots to the right and Table 7.

and nodes within it based on the same average rate are presented in Table 7.

4. Discussion

4.1. Hoplocercinae phylogeny

The multilocus phylogenetic analyses presented here provide the first strongly supported hypothesis of relationships among hoplocercine lizards. Given that strongly supported clades (BP > 90, PP > 95) are fully congruent among the different datasets, we favor the estimate of hoplocercine phylogeny inferred from the combined (i.e., mtDNA + nDNA) dataset. Analyses of the unpartitioned and partitioned (two strategies) versions of the combined dataset yielded identical ingroup tree topologies (Fig. 3). Moreover, the same ingroup topology was obtained from analyses of the mitochondrial dataset (Fig. 2a).

Table 7
Node ages in millions of years based on assuming an average rate of 0.0065 substitutions/site/million years (Macey et al., 1998). For each node the estimated age along with the 95% high posterior density interval (95% HPD) are presented. Node numbers correspond to those in Fig. 6.

Node number	Age	95% (HPD)
1	34.64	28.04–41.67
2	27.38	22.73–32.31
3	22.77	18.24–27.78
4	6.98	5.19–8.95
5	6.28	4.33–8.39
6	24.08	19.76–28.68
7	20.86	16.87–25.01
8	2.91	1.90–4.07
9	16.46	12.89–20.24
10	11.17	8.13–14.28

Monophyly of Hoplocercinae was inferred under maximum-likelihood and Bayesian analyses of all datasets, though only relative to the five outgroups represented in this study (i.e., not necessarily relative to Crotaphytinae, Iguaninae, and Polychrotinae); moreover, except for analyses of the least-informative gene, *BDNF*, it was strongly supported in all cases (Figs. 2 and 3). In contrast, our results suggest that *Enyalioides* may not be monophyletic, which is in agreement with two of the previously proposed hypotheses (Fig. 1a and c). Analyses of the mtDNA (Fig. 2a) and combined (Fig. 3) datasets had *M. annularis* nested within *Enyalioides* as sister to a clade composed of *E. oshaughnessyi*, *E. palpebralis*, *E. microlepis*, *E. praestabilis*, and *E. touzeti*. Analyses of the *BDNF* dataset (Fig. 2b) placed *Hoplocercus* in a clade with *E. laticeps*, *E. oshaughnessyi*, and *E. touzeti*, whereas analyses of the *RAG1* (Fig. 2c) and nDNA (Fig. 2d) datasets were ambiguous with regard to the monophyly of *Enyalioides*. However, the monophyly of *Enyalioides* could not be statistically rejected with the combined dataset (Table 6).

Etheridge and de Queiroz (1988) were the first authors to present a phylogenetic analysis of hoplocercines. According to their results, which were based primarily on discrete morphological characters, *E. laticeps* was the sister taxon to all other hoplocercines, and *Hoplocercus* and *Morunasaurus* were deeply nested within *Enyalioides* (Fig. 1d). More recently Wiens and Etheridge (2003) presented the results of phylogenetic analyses based on morphological data including polymorphic and meristic characters. Their analyses yielded three different topologies based on three different methods of weighting meristic characters (Fig. 1a–c). When tested against the ML tree obtained for the combined mtDNA and nDNA dataset presented in this paper (Fig. 3), all the morphology-based hypotheses were strongly rejected (Table 6).

That all previous phylogenetic hypotheses were markedly different among each other and statistically rejected when compared to the maximum-likelihood and Bayesian trees presented in this paper suggests that the morphological characters used to obtain those hypotheses are phylogenetically misleading, possibly due to high levels of homoplasy (Wiens and Etheridge, 2003). The molecular characters used in the present study are very informative, as indicated by high clade support values (Fig. 3), though the position of *Morunasaurus* remains unclear. In contrast to other ingroup clades, which are strongly supported, inclusion of *Morunasaurus* within *Enyalioides* is only moderately supported by maximum-likelihood and Bayesian (*a priori* partitioned and mixture-models) analyses of the combined mtDNA and nDNA dataset (Fig. 3). We expect that inclusion of more genes, as well as those hoplocercine species that were not available for this study (*E. cofanorum*, *M. groi*, and *M. peruvianus* [nuclear genes]), will help to clarify the phylogenetic position of *Morunasaurus*. Nonetheless, unlike previous hypotheses, relationships among species of *Enyalioides* are strongly supported by all datasets used in this study (Figs. 2a,c,d and 3) except *BDNF* (Fig. 2b), which was not as informative as the other genes/fragments (Table 3). The only similarities between our preferred hypothesis (Fig. 3) and some of the previous hypotheses (in parentheses) are (1) *Hoplocercus* as the sister taxon to a clade composed of *Enyalioides* and *Morunasaurus* (Wiens and Etheridge, 2003 and Fig. 1b), (2) the sister taxon relationship between *E. microlepis* and *E. praestabilis* (Wiens and Etheridge, 2003 and Fig. 1d), and (3) a clade composed of *E. microlepis*, *E. oshaughnessyi*, *E. palpebralis*, and *E. praestabilis* (Wiens and Etheridge, 2003 and Fig. 1c).

4.2. Biogeography and relative divergence times

All species of hoplocercines occur in lowlands. Most species occur east of the Andes, with *E. heterolepis*, *E. oshaughnessyi*, *E. touzeti*, and *M. groi* (not included in our analyses) being the only species known to occur west of the Andes. That those species occurring east of the Andes are deeply nested in our tree (Fig. 5) suggests that the most recent common ancestor (MRCA) of hoplocercines occurred east of the Andes, which is in agreement with a previous hypothesis that the MRCA of Hoplocercinae occurred in the Amazon basin (Wiens and Etheridge, 2003). However, based on the preferred topology of our study (Fig. 3) and the present distribution of the terminal taxa, it remains unclear whether the MRCA of Hoplocercinae occurred in the Amazon basin, the Brazilian Cerrado region, or both. Our results also suggest that western taxa included in our analyses (i.e., *E. heterolepis*, *E. oshaughnessyi*, *E. touzeti*) originated from at least two separate colonizations followed by allopatric speciation (Fig. 6), whether resulting from dispersal or vicariance. Similarly, another allopatric speciation event east of the Andes might explain the split between *E. palpebralis* (Peru, Bolivia, western Brazil) and the clade composed of *E. microlepis* and *E. praestabilis* (Ecuador, Colombia, northern Peru). On the other hand, Wiens and Etheridge (2003) suggested that sister species *E. microlepis* and *E. praestabilis* either speciated sympatrically, or there was dispersal subsequent to speciation. Given that the distributions of these two species overlap only partially, there is currently little evidence for sympatric speciation.

Molecular dating methods have not been widely applied to taxa for which calibration points (i.e., fossil taxa, geological events) are unavailable. In the absence of calibration points, only arbitrary calibrations (e.g., ucld.mean fixed to 1.0) resulting in relative age estimates are possible. These estimates, however, still contain useful information on the relative timing of events. For example, one might be interested in determining whether two radiations occurred at the same time, or if one radiation is significantly older than the other. Species of *Enyalioides* form two well supported clades (setting aside the possible inclusion of *Morunasaurus*), each with a split between western and eastern (relative to the Andes) taxa. Extensive overlap in the estimated divergence times (node height 95% HPD = 0.0792–0.1149 and 0.0786–0.1132 substitution/site for nodes 3 and 7, respectively [partitioned dataset]; Fig. 6) indicates that the split between western and eastern taxa occurred at about the same time in both clades, which suggests that these splits were caused by a common vicariant event that fragmented populations of two ancestral species that had continuous distributions between the present Amazon basin and Pacific coast. Given that most species of hoplocercines occur in the lowlands adjacent to the northern Andes (i.e., northern Peru, Ecuador, Colombia), with no species known from the Pacific coast south of Ecuador, the most obvious geological event to explain this vicariance is the uplift of the northern Andes, assuming that the common ancestors, like all extant species of Hoplocercinae, were restricted to the lowlands. If this is true, there is a wide range of possible dates for the relevant nodes. A single date for the uplift

of the northern Andes is unrealistic because the Andes are not a single entity; uplift did not happen instantaneously, and its timing probably varied latitudinally and longitudinally (Gregory-Wodzicki, 2000). The two splits could be as old as the Late Cretaceous, when the Andes were uplifted to elevations not greatly exceeding 1000 m (Simpson, 1979)—extant hoplocercine species occur mostly below 1000 m except for *E. praestabilis*, which has been found at elevations close to 2000 m (specimen 2156 in the Fundación Herpetológica Gustavo Orcés, Ecuador). However, if this modest Late Cretaceous mountain chain did not represent a geographic barrier to the *Enyalioides* species living at that time, the splits must have occurred more recently when the northern Andes became high enough to be a barrier. The northern Andes, in particular the eastern Cordillera in Colombia, underwent rapid uplift 2–5 million years ago leading to a definitive separation between the Amazonian rain forest and the Chocó region (Van der Hammen et al., 1973; Simpson, 1979; Aleman and Ramos, 2000; Gregory-Wodzicki, 2000). Thus, ages of nodes 3 and 7 could be any time between the Late Cretaceous and the Pliocene; based on a rate of sequence evolution estimated for a group of agamid lizards (Macey et al., 1998), those ages are 22.77 my (95% HPD = 18.24–27.78) and 20.86 my (95% HPD = 16.87–25.01), respectively. Regardless of the accuracy of the estimated absolute ages, the analysis of relative divergence times has allowed us to postulate that a single vicariant event, most likely the uplift of the northern Andes, caused the split between western and eastern taxa in two subclades of *Enyalioides*, thus demonstrating the utility of relative divergence time estimates.

The differences between divergence time estimates obtained using the uncorrelated lognormal method with and without partition-specific parameter estimates indicate that partitioning can have a significant impact on node height (age) estimates. Overall, age estimates were greater for the partitioned dataset (0.01–0.31 substitutions/site, mean = 0.11 ± 0.09 SD) than they were for the unpartitioned dataset (0.01–0.16 substitutions/site, mean = 0.07 ± 0.05 SD). Assuming that data partitioning permits more accurate results in a model-based framework, it appears that failure to partition the data can lead to underestimating numbers of substitutions and thus also divergence times. Moreover, this underestimation is more marked for older nodes (Fig. 6).

4.3. Sequence variation and species limits

Interspecific divergence values are generally, though not necessarily (de Queiroz and Good, 1997), expected to be larger than intraspecific ones. The lowest interspecific divergence values are outliers and correspond to the divergence between *E. oshaughnessyi* (three samples) and *E. touzeti* (one sample), as well as the divergence between *Morunasaurus annularis* and *M. peruvianus*. There is little genetic divergence (maximum-likelihood corrected distance values) among samples of *E. oshaughnessyi* (0.003–0.052), as well as between this species and *E. touzeti* (0.03–0.047; Fig. 4). Moreover, a maximum-likelihood analysis of the expanded mitochondrial dataset placed *E.* sp. within *E. oshaughnessyi* (Fig. 5). Although this finding, in the absence of other information, suggests that *E. touzeti* is conspecific with *E. oshaughnessyi*, there is compelling morphological evidence supporting *E. touzeti* as a separate species (Torres-Carvajal et al., 2008) . Assuming that all samples of *E. oshaughnessyi* included in this study represent a single species, this could be a case of fixed morphological differences evolving prior to the evolution of reciprocal monophyly of mtDNA alleles. On the other hand, if *E. oshaughnessyi* as currently circumscribed represents more than one species, the morphological differentiation of *E. touzeti* would seem to represent fixation of novel morphological characters in one of the lineages but not the others. Both scenarios suggest that the split between the new species and *E. oshaughnessyi* is recent, which is supported by the analysis of relative divergence times (Fig. 6).

Divergence between *M. annularis* and *M. peruvianus* is also low (0.042) for an interspecific comparison. These putative species are very similar morphologically (Köhler et al., 1999; Köhler, 2003). Additional morphological and molecular studies with samples from several populations are necessary to assess the taxonomic status of populations currently recognized as *M. annularis* and *M. peruvianus* more definitively.

Although samples are small, the intraspecific divergence values show some geographic structure. *E. heterolepis* is widely distributed west of the Andes from Panama to Ecuador. Our three samples of this species form a well supported monophyletic group (Fig. 5). Sequences of the two individuals from Panama are more similar to each other (0.025) than they are to an individual from Ecuador (0.063 and 0.068). *E. laticeps* is widely distributed across the western Amazon basin (Avila-Pires, 1995). Our four samples of this species similarly form a strongly supported monophyletic group, with the two individuals from Peru and Brazil more similar to each other (0.049) than they are to either of the two samples from Ecuador (0.069–0.081), which, likewise, are more similar to each other (0.017).

4.4. Phylogenetic nomenclature of Hoplocercinae

In the interest of promoting clarity and precision regarding the names of clades of hoplocercine lizards, we propose phylogenetic definitions (de Queiroz and Gauthier, 1990, 1992, 1994) for three clade names according to the rules of the draft *International Code for Phylogenetic Nomenclature* (*ICPN*, Cantino and de Queiroz, 2007). Although these proposals do not establish the names officially because the ICPN is still in draft form, they nonetheless serve as examples for the future phylogenetic nomenclature of hoplocercine lizards.

Hoplocercinae Macey et al., 1997a (converted clade name). *Definition:* The crown clade originating with the most recent common ancestor of *Enyalioides* (*Enyalus*) *laticeps* (Guichenot, 1855), *E.* (*Enyalius*) *oshaughnessyi* (Boulenger, 1881), *Hoplocercus spinosus* Fitzinger, 1843, *Morunasaurus* (*Hoplocercus*) *annularis* (O'Shaughnessy, 1881), and *Morunasaurus groi* Dunn, 1933. *Reference phylogenies:* Figs. 3 and 6 of this paper. Hypothesized composition: *Enyalioides*, *Hoplocercus*, and *Morunasaurus* (see below). *Diagnostic apomorphies:* see Etheridge and de Queiroz (1988), Frost and Etheridge (1989), and Wiens and Etheridge (2003). *Comments: Hoplocercinae* (Macey et al., 1997a) was selected over several older names for the same clade: hoplocercines (Smith et al., 1973), morunasaurines (Estes and Price, 1973), morunasaurs (Etheridge and de Queiroz, 1988), and *Hoplocercidae* (Frost and Etheridge, 1989). The first three are informal names and thus unavailable for conversion, though the name selected could be interpreted as a Latinized version of the first and oldest. The fourth was not selected because its ending might be misinterpreted as implying mutual exclusivity relative to the more inclusive clade *Iguanidae*. According to the stated definition, the hypothesized composition of *Hoplocercinae* is the same regardless of whether it is applied in the context of the phylogenetic hypothesis supported by the results of the present study (Figs. 3 and 6) or under previously proposed phylogenetic hypotheses (Fig. 1a–d). *Morunasaurus groi* is included as an internal specifier despite not being included in the reference phylogeny to ensure that it is part of *Hoplocercinae* should it be placed as the sister group to a clade formed by all other currently recognized species of hoplocercines.

Enyalioides Boulenger, 1885 (converted clade name). *Definition:* The crown clade originating with the most recent common ancestor of *Enyalioides cofanorum* Duellman, 1973, *E. (Enyalus) heterolepis* (Bocourt, 1874), *E.* (*Enyalus*) *laticeps* (Guichenot, 1855), *E.*

(*Enyalius*) *microlepis* (O'Shaughnessy, 1881), *E.* (*Enyalius*) *oshaughnessyi* (Boulenger, 1881), *E.* (*Enyalius*) *palpebralis* (Boulenger, 1883), *E.* (*Enyalius*) *praestabilis* (O'Shaughnessy, 1881) and *E. touzeti* Torres-Carvajal et al., 2008. *Reference phylogeny:* Figs. 3 and 6 of this paper. *Hypothesized composition: Enyalioides* is currently hypothesized to include the species used as internal specifiers in the definition of the name and possibly *Morunasaurus* (see Comments). *Diagnostic apomorphies:* Wiens and Etheridge (2003) provided putative morphological synapomorphies for two trees on which *Enyalioides* was inferred to be monophyletic. *Comments:* According to the phylogeny inferred in the present study (Figs. 3 and 6), *Morunasaurus* is a subclade of *Enyalioides* rather than a non-overlapping clade, though this relationship is not strongly supported. If *Morunasaurus* is inferred not to be nested within *Enyalioides* and if new species are described that are closer to *Enyalioides* than to *Morunasaurus*, we intend for them to be included within *Enyalioides*. Therefore, if any such species are discovered that are outside of the clade originating from the most recent common ancestor of the currently known *Enyalioides* species, the present definition may be emended to include those species as internal specifiers without petitioning the Committee on Phylogenetic Nomenclature (an unrestricted emendation).

Hoplocercus Fitzinger, 1843 (converted clade name). *Definition:* The most inclusive crown clade exhibiting a depressed, short tail (tail length < snout-vent length), with enlarged spiny scales dorsally and laterally, synapomorphic with that of *Hoplocercus spinosus* Fitzinger, 1843. *Reference phylogeny:* Figs. 3 and 6 of this paper. Hypothesized composition: *Hoplocercus* is currently inferred to contain a single extant species, *H. spinosus*. *Diagnostic apomorphies:* see Etheridge and de Queiroz (1988). *Comments:* A definition based on the apomorphy of a short, spiny tail was chosen so that the name *Hoplocercus* will include any newly discovered or resurrected extant species possessing that apomorphy, in keeping with the etymology of the name (*hoplon* = Gk., armor, shield + *kerkos* = Gk., tail).

Morunasaurus Dunn, 1933 (converted clade name). *Definition:* No formal definition is provided at the present time (see Comments). *Hypothesized composition: Morunasaurus* is hypothesized to include three currently recognized species: *M. groi* Dunn, 1933, *M.* (*Hoplocercus*) *annularis* (O'Shaughnessy, 1881), and *M. peruvianus* Köhler, 2003. Diagnostic apomorphies: Wiens and Etheridge (2003) provided putative morphological synapomorphies for one tree on which *Morunasaurus* was inferred to be monophyletic. *Comments:* We have chosen not to provide a formal definition for the name *Morunasaurus* because we have not sampled the type species (*M. groi*) and therefore cannot confirm that it is closely related to *M. annularis* and *M. peruvianus*.

Acknowledgments

For the loan of tissue samples we thank A. Almendáriz (EPN), L.A. Coloma (QCAZ), J. Córdoba, and C. Aguilar (MHNSM), R. Ibáñez (CH), L. Trueb (KU), J. Valencia (FHGO), H. Zaher (MZUSP), and all individuals involved in the collection of these samples. Lab supplies and equipment were provided by the Laboratories of Analytical Biology of the Smithsonian Institution. J.A. Schulte and T. Townsend provided helpful lab advice. A. Meade and M. Pagel kindly shared a test version of BayesPhylogenies that includes reversible jump Markov Chain Monte Carlo. A. Rambaut clarified the interpretation of time when the mean of branch rates parameter is set to 1 in BEAST.

Appendix A. Supplementary data

Supplementary data associated with this article can be found, in the online version, at doi:10.1016/j.ympev.2008.10.002.

References

Aleman, A., Ramos, V.A., 2000. Northern Andes. In: Cordani, U.G., Milani, E.J., Thomaz-Filho, A., Campos, D.A. (Eds.), Tectonic Evolution of South America. Brazilian Academy of Science, Rio de Janeiro, pp. 453–480.
Avila-Pires, T.C.S., 1995. Lizards of Brazilian Amazonia (Reptilia: Squamata). Natl. Nat. Mus. Zool. Verh. 299, 1–706.
Bocourt, M.F., 1874. Notes sur quelques sauriens de l'Amerique tropicale. Ann. Sci. Nat. Paris 19, 1–2.
Boulenger, G.A., 1881. Description of a new species of *Enyalius* in the Brussels museum. Proc. Zool. Soc. Lond. 1, 246–247.
Boulenger, G.A., 1883. Description of a new species of lizard of the genus *Enyalius*. Proc. Zool. Soc. Lond. 1, 46.
Boulenger, G.A., 1885. Catalogue of the lizards in the British Museum (Natural History) II. Taylor and Francis, London.
Burnham, K.P., Anderson, D.R., 2004. Multimodel inference. Understanding AIC and BIC in model selection. Sociol. Methods Res. 33, 261–304.
Cantino, P.D., de Queiroz, K., 2007. PhyloCode: A Phylogenetic Code of Biological Nomenclature. Version 4b. Available from: <http://www.ohiou.edu/phylocode/>.
de Queiroz, K., Gauthier, J., 1990. Phylogeny as a central principle in taxonomy: phylogenetic definitions of taxon names. Syst. Zool. 39, 307–322.
de Queiroz, K., Gauthier, J., 1992. Phylogenetic taxonomy. Annu. Rev. Ecol. Syst. 23, 449–480.
de Queiroz, K., Gauthier, J., 1994. Toward a phylogenetic system of biological nomenclature. Trends Ecol. Evol. 9, 27–31.
de Queiroz, K., Good, D.A., 1997. Phenetic clustering in biology: a critique. Q. Rev. Biol. 72, 3–30.
Drummond, A.J., Rambaut, A., 2007. BEAST: Bayesian evolutionary analysis by sampling trees. BMC Evol. Biol. 7, 214.
Drummond, A.J., Ho, S.Y.W., Phillips, M.J., Rambaut, A., 2006. Relaxed phylogenetics and dating with confidence. PLOS Biol. 4, 699–710.
Duellman, W.E., 1973. Descriptions of new lizards from the upper Amazon basin. Herpetologica 29, 228–231.
Dunn, E.R., 1933. Amphibians and reptiles from El Valle de Anton, Panama. Occas. Pap. Boston Soc. Nat. Hist. 8, 65–79.
Estes, R., Price, L.I., 1973. Iguanid lizard from the Upper Cretaceous of Brazil. Science 180, 748–751.
Etheridge, R., 1969. A review of the iguanid lizard genus *Enyalius*. Bull. Brit. Mus. Nat. Hist. (Zool.) 18, 231–260.
Etheridge, R., de Queiroz, K., 1988. A phylogeny of Iguanidae. In: Estes, R., Pregill, G. (Eds.), Phylogenetic Relationships of the Lizard Families. Stanford University Press, Stanford, pp. 283–367.
Fitzinger, L.I., 1843. Systema Reptilium, Fasciculus Primus, Amblyglossae. Baumüller und Seidel, Wien.
Frost, D.R., Etheridge, R., 1989. A phylogenetic analysis and taxonomy of iguanian lizards (Reptilia: Squamata). Misc. Pub. Univ. Kans. Nat. Hist. Mus. 81, 1–65.
Gelman, A., Rubin, D.B., 1992. Inference from iterative simulation using multiple sequences. Stat. Sci. 7, 457–511.
Gregory-Wodzicki, K.M., 2000. Uplift history of the central and northern Andes: a review. Geol. Soc. Am. Bull. 112, 1091–1105.
Guichenot, A., 1855. Reptiles. In: de Castelnau F. (Ed.), Animaux nouveaux ou rares recueillis pendant l'expédition dans les parties centrales de l'Amérique du Sud, de Rio de Janeiro a Lima, et de Lima au Para; exécutée par ordre du gouvernement français pendant les années 1843 a 1847, sous la direction du Comte Francis de Castelnau. Chez P. Bertrand, Libraire-Éditeur, Paris, pp. 1–95.
Huelsenbeck, J.P., Ronquist, F., 2001. MrBayes: Bayesian inference of phylogeny. Bioinformatics 17, 754–755.
Huelsenbeck, J.P., Larget, B., Alfaro, M.E., 2004. Bayesian phylogenetic model selection using reversible jump Markov chain Monte Carlo. Mol. Biol. Evol. 21, 1123–1133.
Kass, R.E., Raftery, A.E., 1995. Bayes factors. J. Am. Stat. Assoc. 90, 773–795.
Köhler, G., Seipp, R., Moya, S., Almendáriz, A., 1999. Zur Kenntnis von *Morunasaurus annularis* (O'Shaughnessy, 1881). Salamandra 35, 181–190.
Köhler, G., 2003. A new species of *Morunasaurus* from Peru (Reptilia, Squamata, Hoplocercidae). Senckenb. Biol. 82, 235–241.
Kumazawa, Y., Nishida, M., 1993. Sequence evolution of mitochondrial tRNA genes and deep-branch animal phylogenetics. J. Mol. Evol. 37, 380–398.
Leaché, A.D., McGuire, J.A., 2006. Phylogenetic relationships of horned lizards (*Phrynosoma*) based on nuclear and mitochondrial data: evidence for a misleading mitochondrial gene tree. Mol. Phylogenet. Evol. 39, 628–644.
Leviton, A.E., Gibbs, R.H., Heal, E., Dawson, C.E., 1985. Standards in herpetology and ichthyology: part I. Standard symbolic codes for institutional resource collections in herpetology and ichthyology. Copeia 1985, 802–832.
Macey, J.R., Larson, A., Ananjeva, N.B., Papenfuss, T.J., 1997a. Evolutionary shifts in three major structural features of the mitochondrial genome among iguanian lizards. J. Mol. Evol. 44, 660–674.
Macey, J.R., Larson, A., Ananjeva, N.B., Fang, Z., Papenfuss, T.J., 1997b. Two novel gene orders and the role of light-strand replication in rearrangement of the vertebrate mitochondrial genome. Mol. Biol. Evol. 14, 91–104.
Macey, J.R., Schulte II, J.A., Ananjeva, N.B., Larson, A., Rastegar-Pouyani, N., Shammakov, S.M., Papenfuss, T.J., 1998. Phylogenetic relationships among Agamid lizards of the *Laudakia caucasia* species group: testing hypotheses of biogeographic fragmentation and an area cladogram for the Iranian Plateau. Mol. Phylogenet. Evol. 10, 118–131.

Macey, J.R., Schulte II, J.A., Larson, A., Tuniyev, B.S., Orlov, N., Papenfuss, T.J., 1999. Molecular phylogenetics, tRNA evolution, and historical biogeography in anguid lizards and related taxonomic families. Mol. Phylogenet. Evol. 12, 250–272.

Macey, J.R., Verma, A., 1997. Re: homology in phylogenetic analysis: alignment of transfer RNA genes and the phylogenetic position of snakes. Mol. Phylogenet. Evol. 7, 272–279.

Maddison, D.R., Maddison, W.P., 2001. MacClade: Analysis of Phylogeny and Character Evolution. Version 4.03. Sinauer Associates, Sunderland.

Noonan, B.P., Chippindale, P.T., 2006. Vicariant origin of Malagasy reptiles supports late cretaceous Antarctic land bridge. Am. Nat. 168, 730–741.

O'Shaughnessy, A.W.E., 1881. An account of the collection of lizards made by Mr. Buckley in Ecuador, and now in the British Museum, with descriptions of the new species. Proc. Zool. Soc. Lond. 1881, 227–245.

Pagel, M., Meade, A., 2004. A phylogenetic mixture model for detecting pattern-heterogeneity in gene sequence or character-state data. Syst. Biol. 53, 571–581.

Pagel, M., Meade, A., 2005. Mixture models in phylogenetic inference. In: Gascuel, O. (Ed.), Mathematics of Evolution and Phylogeny. Clarendon Press, Oxford, pp. 1–22.

Posada, D., Crandall, K.A., 1998. Modeltest: testing the model of DNA substitution. Bioinformatics 14, 817–818.

Raftery, A.E., 1996. Hypothesis testing and model selection. In: Gilks, W.R., Richardson, S., Spiegelhalter, D.J. (Eds.), Markov Chain Monte Carlo in Practice. Chapman and Hall, London, pp. 163–187.

Rambaut, A., Drummond, A.J., 2007. Tracer. Version 1.4. Available from: <http://beast.bio.ed.ac.uk/Tracer/>.

Ripplinger, J., Sullivan, J., 2008. Does choice in model selection affect maximum likelihood analysis? Syst. Biol. 57, 76–85.

Ronquist, F., Huelsenbeck, J.P., 2003. MrBayes 3: Bayesian phylogenetic inference under mixed models. Bioinformatics 19, 1572–1574.

Schulte, J.A., de Queiroz, K., 2008. Phylogenetic relationships and heterogeneous evolutionary processes among phrynosomatine sand lizards (Squamata, Iguanidae) revisited. Mol. Phylogenet. Evol. 47, 700–716.

Schulte II, J.A., Macey, J.R., Larson, A., Papenfuss, T.J., 1998. Molecular tests of phylogenetic taxonomies: a general procedure and example using four subfamilies of the lizard family Iguanidae. Mol. Phylogenet. Evol. 10, 367–376.

Schulte II, J.A., Macey, J.R., Espinoza, R.E., Larson, A., 2000. Phylogenetic relationships in the iguanid lizard genus *Liolaemus*: multiple origins of viviparous reproduction and evidence for recurring Andean vicariance and dispersal. Biol. J. Linn. Soc. 69, 75–102.

Schulte II, J.A., Valladares, J.P., Larson, A., 2003. Phylogenetic relationships within Iguanidae inferred using molecular and morphological data and a phylogenetic taxonomy of iguanian lizards. Herpetologica 59, 399–419.

Shimodaira, H., Hasegawa, M., 1999. Multiple comparisons of log-likelihoods with applications to phylogenetic inference. Mol. Biol. Evol. 16, 1114–1116.

Shimodaira, H., 2002. An approximately unbiased test of phylogenetic tree selection. Syst. Biol. 51, 492–508.

Shimodaira, H., Hasegawa, M., 2001. CONSEL: for assessing the confidence of phylogenetic tree selection. Bioinformatics 17, 1246–1247.

Simpson, B.B., 1979. Quaternary biogeography of the high montane regions of South America. In: Duellman, W.E. (Ed.), The South American Herpetofauna: Its Origin, Evolution and Dispersal. University of Kansas Natural History Museum, Lawrence, pp. 157–188.

Smith, H.M., Sinelnik, G., Fawcett, J.D., Jones, R.E., 1973. A survey of the chronology of ovulation in anoline lizard genera. Trans. Kans. Acad. Sci. 75, 107–120.

Sullivan, J., Abdo, Z., Joyce, P., Swofford, D.L., 2005. Evaluating the performance of a successive-approximations approach to parameter optimization in maximum-likelihood phylogeny estimation. Mol. Biol. Evol. 22, 1386–1392.

Swofford, D.L., 2003. PAUP*. Phylogenetic Analysis Using Parsimony* (and other methods). Version 4.0. Sinauer Associates, Sunderland.

Swofford, D.L., Olsen, G.J., Waddell, P.J., Hillis, D.M., 1996. Phylogenetic inference. In: Hillis, D.M., Moritz, C., Mable, B.K. (Eds.), Molecular Systematics, second ed. Sinauer Associates, Sunderland, pp. 407–543.

Thompson, J.D., Gibson, T.J., Plewniak, F., Jeanmougin, F., Higgins, D.G., 1997. The ClustalX windows interface: flexible strategies for multiple sequence alignment aided by quality analysis tools. Nucleic Acids Res. 24, 4876–4882.

Torres-Carvajal, O., Schulte II, J.A., Cadle, J.E., 2006. Phylogenetic relationships of South American lizards of the genus *Stenocercus* (Squamata: Iguania): a new approach using a general mixture model for gene sequence data. Mol. Phylogenet. Evol. 39, 171–185.

Torres-Carvajal, O., Almendáriz, A., Valencia, J., Yánez-Muñoz, M., Reyes, J.P., 2008. A new species of *Enyalioides* (Iguanidae: Hoplocercinae). Pap. Avul. Zool. 48, 227–235.

Townsend, T., Larson, A., Louis, E., Macey, J.R., 2004. Molecular phylogenetics of Squamata: the position of snakes, amphisbaenians, and dibamids, and the root of the squamate tree. Syst. Biol. 53, 735–757.

Van der Hammen, T., Werner, J.H., Van Dommelen, H., 1973. Palynological record of the upheaval of the northern Andes: a study of the Pliocene and lower quaternary of the Colombian eastern Cordillera and the early evolution of its high-Andean biota. Rev. Palaeobot. Palynol. 16, 1–122.

Vitt, L.J., de la Torre, S., 1996. Guía para la investigación de las lagartijas de Cuyabeno. A research guide to the lizards of Cuyabeno. Museo de Zoología (QCAZ), Centro de Biodiversidad y Ambiente, Pontificia Universidad Católica del Ecuador. Monografía 1, 1–165.

Weisrock, D.W., Macey, J.R., Ugurtas, I.H., Larson, A., Papenfuss, T.J., 2001. Molecular phylogenetics and historical biogeography among salamandrids of the "true" salamander clade: rapid branching of numerous highly divergent lineages in *Mertensiella luschani* associated with the rise of Anatolia. Mol. Phylogenet. Evol. 18, 434–448.

Wiens, J.J., Etheridge, R.E., 2003. Phylogenetic relationships of hoplocercid lizards: coding and combining meristic, morphometric, and polymorphic data using step matrices. Herpetologica 59, 375–398.

Zwickl, D.J., 2006. Genetic Algorithm Approaches for the Phylogenetic Analysis of Large Biological Sequence Datasets under the Maximum likelihood Criterion. Ph.D. Dissertation. The University of Texas at Austin.